Multifrequency Electromagnetic Signature of the Cloud Chamber, Nevada Test Site

Dean Keiswetter and I.J. Won
Geophex, Ltd.
Raleigh, North Carolina

ABSTRACT

Multifrequency electromagnetic (EM) data acquired over the Cloud Chamber (CC), Nevada Test Site (NTS), clearly delineate the lateral bounds of the facility and detect the line-of-sight pipe - a 0.4-m diameter stainless-steel pipe buried nine meters below ground level. The purpose of the ground-based electromagnetic surveys was to demonstrate that the CC could be detected using the GEM-2, and acquire multi-frequency data for inversion processing and algorithm development. We present herein GEM-2 data acquired at the CC and discuss the importance of wideband EM data.

Introduction

Geophex acquired broadband electromagnetic data over the Cloud Chamber (CC) facility, Nevada Test Site (NTS), during 1995 and 1996 to support a Department of Energy (DOE) funded, multi-year, multi-agency research program to geophysically characterize underground structures. This manuscript presents contoured maps of multifrequency EM data and describes the sensor and acquisition methods. Witten et al. (1997) presents details of multifrequency-based inversion theory, and imaging results of these data.

Cloud Chamber

The CC is located in north central Yucca Flats, an alluvial basin on the NTS that has been used repeatedly for underground nuclear tests (Office of External Affairs, 1988). The shallow geologic strata are composed of Tertiary and Quaternary volcanic and clastic rocks (Dockery et al., 1985).

The CC, built in 1968 as part of a diagnostics experimental program, was used to measure ionized particles from the 7.4-kiloton (KT) HUPMOBILE event (Office of External Affairs, 1988). The quonset hut CC structure is approximately 42 m in length, 10 m wide at its base, and 5 m high at its maximum. Semicircular steel members support a wooden frame as shown in fig. 1. The reinforced-concrete floor of the CC is 9 m below ground surface.

Multifrequency Electromagnetic Approach

The electromagnetic induction method can be used to target different depths of interest by changing either the spacing between transmitter and receiver coils, or the frequency of the transmitted field (Patra and Mallick, 1980; Won, 1980). The first method is known as geometrical sounding and involves recording data using several transmitter-receiver coil spacings centered over fixed location; the depth of exploration increases with the coil spacing. The two coils systems, although typically connected by an umbilical cord, are physically separate and require two or more field operators.

The second method is known as frequency sounding and involves changing the transmitter frequency, but keeping the transmitter-receiver separation constant (fig. 2). The depth of exploration (also called the depth of penetration or skin depth) is mainly determined by the source frequency and ground conductivity (Won, 1980). In simple terms, low frequency signals travel further than high frequencies through conductive media and, thus, detect deep structures. Conversely, high frequencies detect shallow features better than low frequencies. Broadband frequency sounding is therefore analogous to depth sounding and can be used to create a pseudo 3-D subsurface image (Won, 1983) or for 3-D conductivity inversion processing (Lee et al., 1987; Witten et al., 1997).

Frequency sounding possesses inherent advantages over geometric sounding for depth imaging because it is logistically and operationally simple (due to a one-person operation) and improves spatial resolution (by averaging vertically instead of laterally; fig. 2). Theoretical and practical discussions on these methods may be found in Grant and West (1965), Keller and Frischkneckt (1966), and Kaufman and Keller (1983).

GEM-2 Sensor and Data Acquisition Methods

We acquired broadband electromagnetic data using the GEM-2, (fig. 3; Won et al., 1996), a multifrequency induction sensor developed at Geophex. The GEM-2 contains a transmitter, receiver, and bucking coil in a single lightweight, portable, and compact package. The signal-processing electronics, analog circuitry (for signal conditioning), and power supply are housed in a removable console.

The primary field generated by the GEM-2 sensor is controlled via a digitally constructed waveform. The transmitted signal can vary from a complex waveform containing any number of frequencies (user-defined) to a simple square wave. Although the design of the GEM-2 allows it to operate in the either the time- or frequency-domain, only frequency domain data were recorded during this project. The maximum current

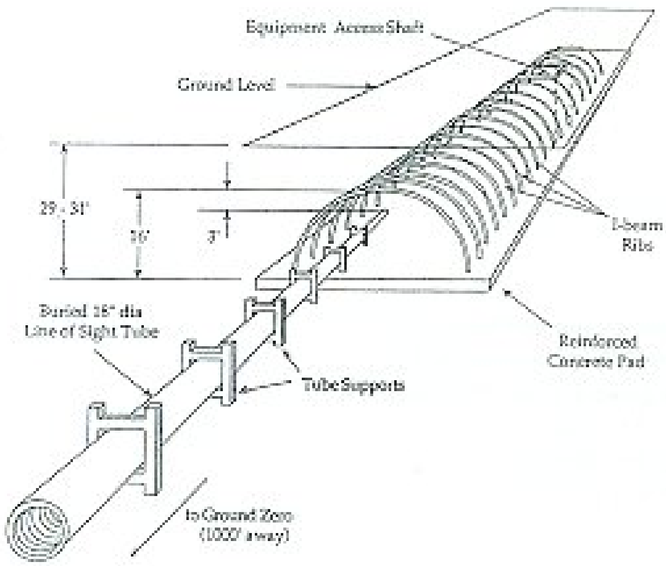

Figure 1. Sketch of the Cloud Chamber (after Kane and Warshaw, 1995).

for the present transmitter is six amperes, corresponding to a dipole moment of about 3 A-m2.

The GEM-2 digitizes and stores signal from the bucking and receiver coil simultaneously at a rate of 48 kHz. A narrow-band, match-filter signal detection technique is used to extract the in-phase and quadrature components. The nominal sampling rate for simultaneous, multifrequency acquisition for earlier GEM-2s was two Hz. Recent improvements to the hardware and software have increased the sampling rate to 10 Hz. A single digital signal processing (DSP) chip coordinates all controls and computations for both transmitter and receiver circuits.

The GEM-2 can transmit and record multiple frequencies simultaneously, as described by Won et al., (1996) or step through a user-defined frequency band, one frequency at a time. For the frequency stepping mode, the GEM-2 computes and transmits a single-frequency square-wave signal, records the primary and secondary field responses, calculates the strength of the induced magnetic field (in parts-per-million), and stores the result internally. The start frequency, end frequency, step size (in Hz), samples length, and numbers of sweeps to perform automatically are field programmable. Current restrictions imposed by the GEM-2 sensor include a minimum start frequency of 90 Hz, Nyquist frequency of 24 kHz, and minimum step size of 30 Hz. The primary advantage of stepping through a given frequency band is to increase the transmitter moment and, consequently, the signal-to-noise ratio.

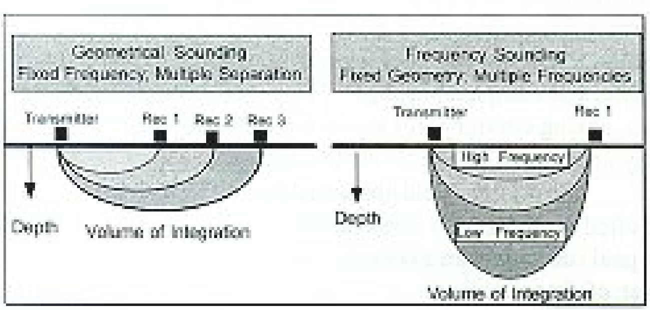

Figure 2. Cartoon of depth sounding techniques using geometrical- and frequency-based methods.

Both methods of data acquisition (i.e., simultaneous multi-frequency and stepped modes) were used during this project.

Electromagnetic Data

Three EM surveys, each with specific goals, were conducted over portions of a 400-foot by 600-foot area that encompasses the CC (fig. 4). The objectives, acquisition techniques, and results of each survey are described below.

Data processing included assigning spatial registry information, kriging (contouring), and display. Two maps, representing the in-phase and quadrature components, are gen-

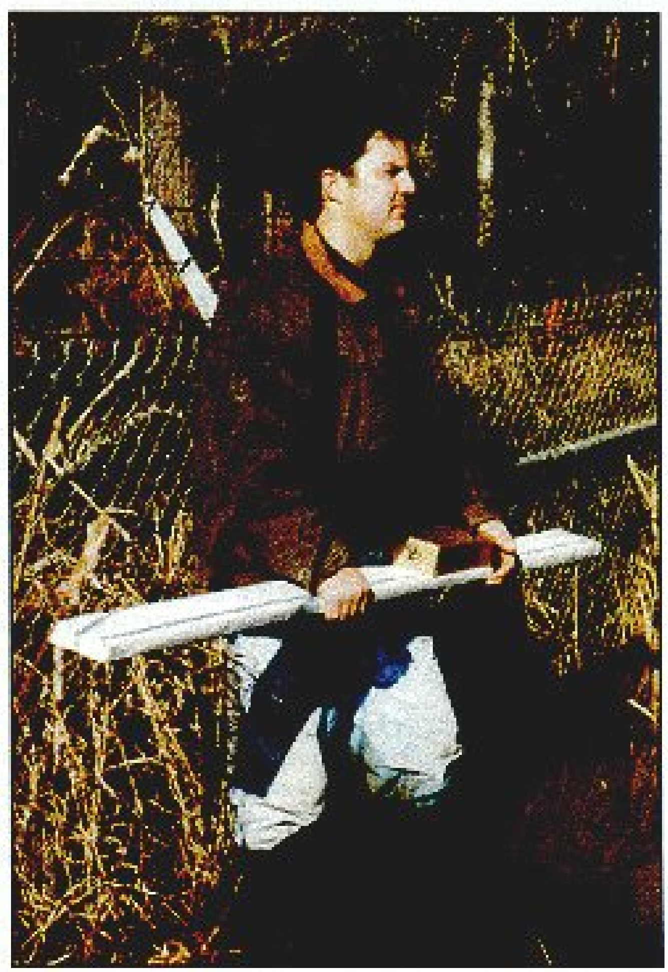

Figure 3. Photograph of the GEM-2 sensor during a recent (non-related) project.

erated for each frequency. Although the multi-frequency data can be converted to apparent conductivity as described by Won et al. (1996), these data are presented in terms of the part-per-million (ppm) response (raw data logged by the GEM-2). The measured ppm response is defined as:

$$ppm = 10^6 \times \frac{\textit{secondary magnetic field at receiver coil}}{\textit{primary magnetic field at receiver coil}}.$$

Survey 1

The objective of the first survey was to demonstrate that the CC could be detected using GEM-2 and facilitate comparisons of the EM results to ancillary geophysical methods (Bartel et al., 1997).

Data were collected over approximately five acres directly above the CC (fig. 4) using seven transmitter frequencies (450, 810, 1,350, 2,430, 4,050, 7,290, and 12,150 Hz) in a vertical-magnetic-dipole (VMD) configuration. Survey lines were spaced five feet apart. Along a survey line, the data were acquired using the dead-reckoning method. This method of assigning spatial registry information to the geophysical data involves acquiring data at equal-time intervals while walking between two known endpoints at a constant pace. Each data sample is assigned spatial coordinates by linearly interpolating between the two end points based on the number of samples. Data were downloaded to a laptop computer and plotted on site for quality checks.

The EM data identify the lateral extent of the CC at all frequencies (fig. 5). The size, orientation, and location of the CC correspond with a prior knowledge. In addition to anoma-

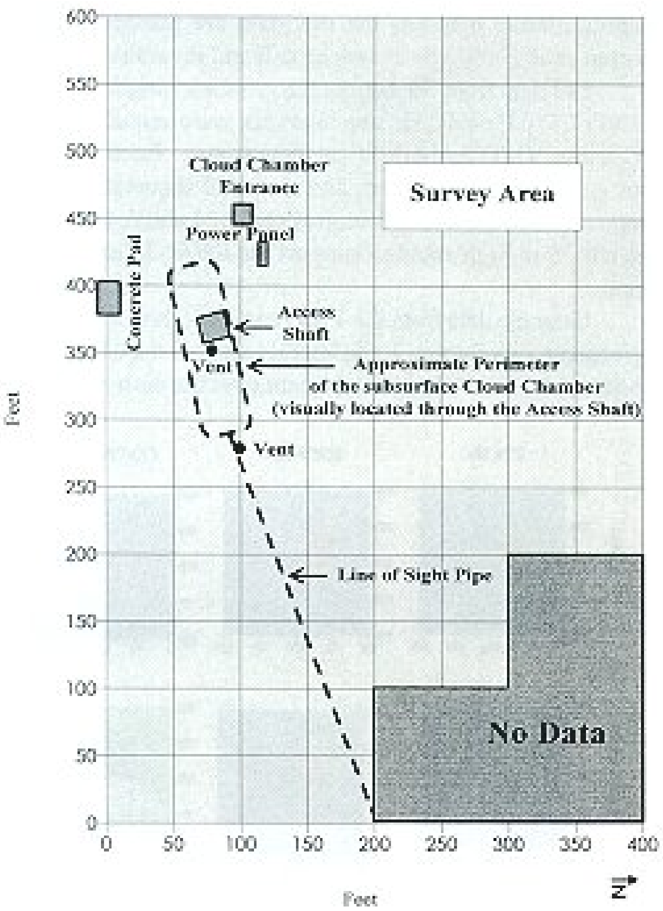

Figure 4. General site map showing grid convention, data coverage, and surficial features. All subsequent data use this coordiante scheme.

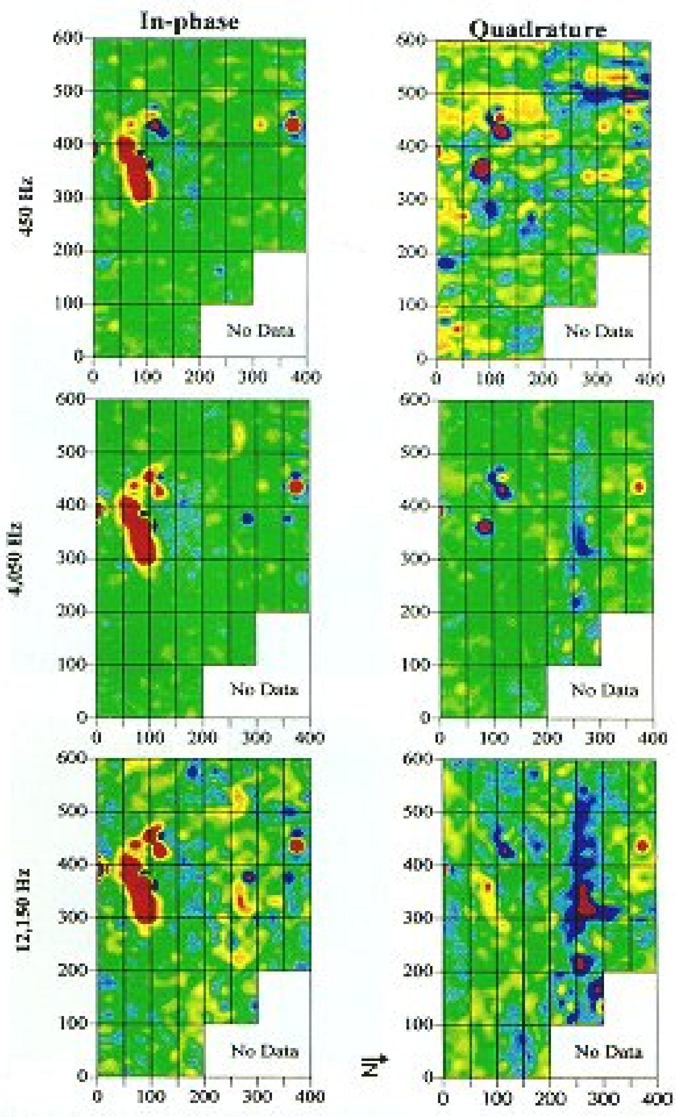

Figure 5. GEM-2 data for selected frequencies from Survey 1. Distances are in feet.

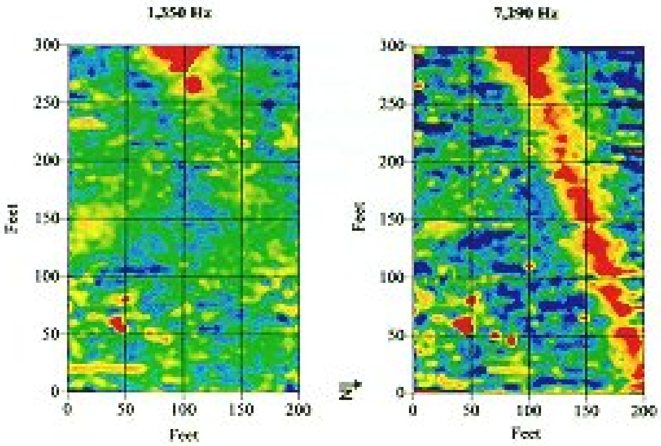

Figure 6. GEM-2 data, acquired using a horizontal dipole configuration, from Survey 2; in-phase component.

lies generated by the CC and surface features (fig. 4), local anomalies are also observed for particular frequencies. Thus, single-frequency EM measurements are insufficient to properly characterize the site.

The CC and supporting structures are best observed in the in-phase component (fig. 5). The quadrature component, which theoretically responds to poor conductors, identifies geological variations within the survey area.

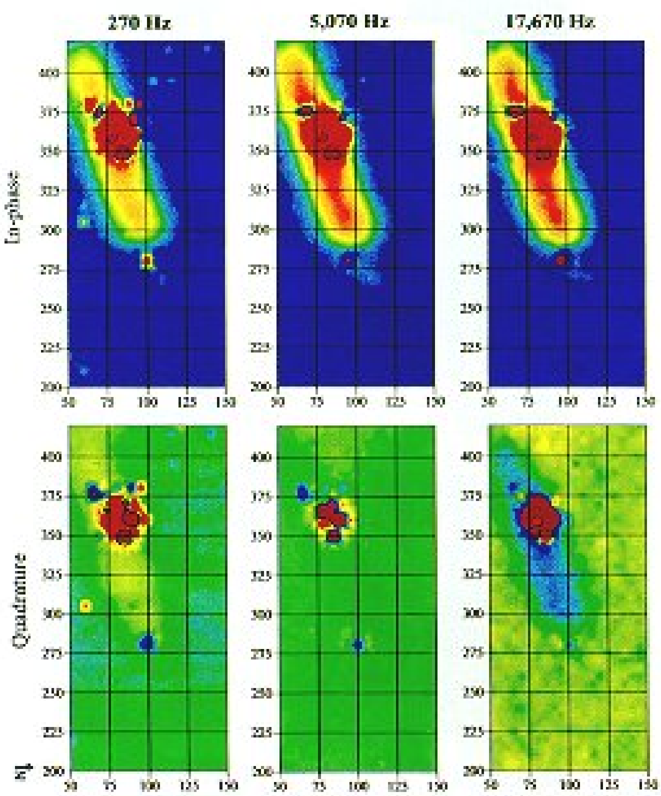

Figure 7. Example GEM-2 data acquired using a vertical magnetic dipole configuration from Survey 3. Distances are in feet.

Survey 2

The target of the second survey was a buried pipe, known as the line-of-sight pipe, that extends northeast from the CC to the HUPMOBILE crater. The line-of-sight pipe is stainless steel, 0.4-m diameter, and buried nine meters below ground level.

Data were acquired, using five-foot line spacing and two transmit frequencies (1,350 and 7,290 Hz), over the eastern portion of the site using a horizontal-dipole-configuration (HMD). The long axis of the ski was orientated parallel to the pipe (roughly east west) in order to maximize the electromagnetic coupling. Note that data acquired using a VMD configuration, shown in fig. 5, and a HMD configuration perpendicular to the pipe (not shown) do not detect the buried pipe.

Figure 6 shows the in-phase response for both frequencies. Note that although the pipe is observed for a transmitter frequency of 7,290 Hz, it is not seen at the lower frequency (1,350 Hz; fig.6) or for the VMD configuration (fig. 5). These data demonstrate the importance of acquisition parameters.

Survey 3

The objective of the third survey was to acquire EM data over a wide frequency band for inversion processing. Representative maps of the raw data are presented below. Witten et al. (1997) discusses broadband inversion theory.

EM data from 30 distinct frequencies, ranging from 270 Hz to 17,670 Hz (600 Hz step interval), were acquired over the CC using VMD and HMD configurations. Each frequency was generated, transmitted, and recorded sequentially. Data were acquired on a five-foot grid centered above the CC, using a 0.75-m high stand to support the GEM-2 during operation.

Example data from the VMD survey is shown in fig. 7. In agreement with Survey 1, the lateral extent of the CC is clearly observed in the in-phase component over the entire frequency

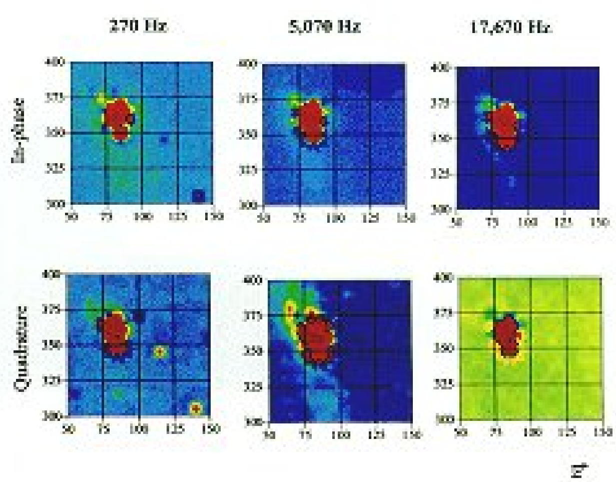

Figure 8. Example GEM-2 data, acquired using horizontal magnetic dipole configuration, from Survey 3. Distances are in feet.

band (fig. 7; top). The quadrature response of the CC shows a phase change such that at low frequencies it is represented by a positive anomaly and at high frequencies it is negative (fig. 7; bottom). The surface vent located at the eastern end of the CC (fig. 4) also shows a frequency-dependent signature [located in fig. 7 at coordinate (100,280)].

Example data acquired using a HMD configuration are shown in fig. 8. These data are dominated by the anomaly associated with the access shaft (fig. 4) that is centered at (80,360).

Conclusions

This data-acquisition project demonstrates that multi-frequency electromagnetic data can successfully delineate the lateral bounds of the CC facility and identify the 9-m deep, 0.4-m diameter, line-of-sight pipe. The frequency-dependent signatures of the CC, isolated anomalies, and geological variations clearly indicate the need for broadband EM surveying.

Data from the line-of-sight pipe confirm the need to utilize prior knowledge when searching for a known target. As demonstrated here, linear conductors are maximally coupled (electromagnetically) with horizontal dipole configurations and may be undetected using a vertical dipole configuration.

The GEM-2 sensor acquires broadband EM data over a field-programmable frequency band. It requires a single operator, is non-intrusive, and can operate at standoff distances. The frequency band, currently restricted to frequencies between 90 and 24 kHz, is suitable for characterization of many environmental and geotechnical applications including mapping underground storage tanks, landfill and trench boundaries, and conductive contaminant plumes. Sensor advancements are currently underway to increase the frequency band, transmitter moment, and sample rate.

Acknowledgments

This project was funded in part by the Los Alamos National Laboratory (Sub contract 2776M0004-8N) and the Oak Ridge National Laboratory (Subcontract 1DY-JEK36V). We thank Dr. Carl Veith (DOE), Dr. Steve Norton (Oak Ridge National Laboratory), Dr. Allen Cogbill (Los Alamos National Laboratory), and Mr. Steve Curtis (DOE) for technical and logistical assistance.

References

Bartel, L., Cress, D., and Stolarcyzk, L., 1997, Evaluation of the electromagnetic gradiometer concept for detection of underground structures - theory and application, Journal of Environmental and Engineering Geophysics, 2, pp. 127-138.

Dockery, H., Byers, F., and Orkild, P., 1985, Nevada Test Site field trip guidebook 1984, Los Alamos National Laboratory, LA-10428-MS, Los Alamos, New Mexico.

Grant, F. S., and West, G. F., 1965, Interpretation theory in applied geophysics, McGraw-Hill, New York.

Kaufman, A. A., and Keller, G. V., 1983, Frequency and Transient Soundings, Elsevier Publishing, Amsterdam.

Kane, R., and Warshaw, S., 1995, A first-look summary of the airborne magnetic field measurements for the WSMR and NTS operations, Lawrence Livermore National Laboratory Report, UCRL-ID-120005, 18 January.

Keller, G. V., and Frischknecht, F. C., 1966, Electrical Methods in Geophysical Prospecting, Pergamon Press, New York.

Lee, S., McMechan, G., and Aiken, C., 1987, Phase-field imaging: The electromagnetic equivalent of seismic migration, Geophysics, **52**, pp. 678-693.

Patra, H. P., and Mallick, K., 1980, Geosounding Principles 2, Elsevier Scientific Publishing Company, New York.

Office of External Affairs, 1988, Announced United States Nuclear Tests, U.S. Department of Energy, NVO-209, rev. 8.

Witten, A., Won, I.J., and Norton, S., 1997, Imaging underground structures using broadband electromagnetic induction, Journal of Environmental and Engineering Geophysics, **2**, pp. 105-114.

Won, I.J., 1980, A wide-band electromagnetic exploration method: Some theoretical and experimental results, Geophysics, **45**, pp. 928-940.

Won, I.J., 1983, A sweep-frequency electromagnetic exploration method, in Development of Geophysical Exploration Methods, Fitch, E., Ed, Elsevier Applied Science Publishers, Ltd., London, pp. 39-64.

Won, I.J., Keiswetter, D., Fields, G., and Sutton, L., 1996, GEM-2: A new multifrequency electromagnetic sensor, Journal of Environmental and Engineering Geophysics, **1**, pp. 129-137.